



Formation and annealing behavior of defect clusters in electron or He-ion irradiated Ti-rich Ti–Al alloys

K. Nakata^{a,*}, K. Fukai^b, A. Hishinuma^b, K. Ameyama^c

^a *The Second Department of Materials, Hitachi Research Laboratory, Hitachi Ltd., Hitachi-shi, Ibaraki 317, Japan*

^b *Department of Materials and Engineering, JAERI, Tokai-mura, Ibaraki 319-11, Japan*

^c *Department of Mechanical Engineering, Faculty of Science and Engineering, Ritsumeikan University, Kusatsu-shi, Shiga 525, Japan*

Received 31 July 1995; accepted 17 September 1996

Abstract

In order to clarify the effect of He atoms on the formation and annealing behavior of defect clusters in Ti–Al alloys, a Ti–47 at.% Al intermetallic compound has been irradiated with electrons and He-ions. Helium-ion irradiation enhances the nucleation of defect clusters, especially of interstitial loops, at temperatures from 623 to 773 K in both γ -TiAl and α_2 -Ti₃Al grains of the sample. However, there is little difference between the annealing temperature ranges of defect clusters in TiAl grains formed by He-ion or electron irradiation at 623 K. The dot-shaped clusters and interstitial loops grow scarcely during annealing, but are annihilated by annealing up to 923 K. Cavities are formed after irradiation with He-ions below 10 dpa at 773 K, but no cavities are formed by electron irradiation up to 30 dpa. The cavities in γ -TiAl and α_2 -Ti₃Al grains survive after annealing even at 1053 K for 1.8 ks, keeping their density and diameter to be nearly the same as those in the as-irradiated grains.

1. Introduction

TiAl intermetallic compounds are attracting much attention in their application to airplane and space materials because of their large strength-to-weight ratio (for a review paper, see [1]). Recently, their use in nuclear reactors has been considered, because both Ti and Al are elements with low neutron-induced radioactivity and small cross-sections of neutron absorption, compared with conventional nuclear materials such as austenitic stainless steels [2]. Before structural applications can be made, however, it is necessary to clarify the radiation resistance of the TiAl compounds and improve their ductility.

Only limited studies on radiation effects have been carried out for these intermetallic compounds. Analysis of microstructural development under electron irradiation suggested TiAl compounds have excellent radiation resistance above 773 K [3–5].

As for mechanical properties of TiAl compounds, neutron irradiation up to about 10^{24} n/m² at 498 K led to an about 10% increase in hardness [6]. It has also been reported that the strength of TiAl increased as a result of proton or Ar-ion irradiation at 98–138 K [7]. Very recently, ductilization from 6.0 to 10.3%, without an increase in yield strength, was found in a Ti–47 at.% Al compound after neutron irradiation at 873 K to 1×10^{24} n/m² [8]. On the other hand, significant ductility loss was reported in a Ti–50 at.% Al compound irradiated with a 1.6×10^{26} n/m² neutron fluence at 673–873 K [9].

For fusion reactor applications, the effect of He on radiation damage in TiAl intermetallic compounds might be important as in austenitic stainless steels. The He generation rates under a 1 MW/m² condition are roughly estimated to be about 7×10^{-6} and 5×10^{-6} appm/s in γ -TiAl and α_2 -Ti₃Al, respectively, based on Santoro's data [10]; these rates are approximately equivalent to that of type 316 stainless steel, that is about 5×10^{-6} appm/s. Therefore, the effect of He can not be neglected in the radiation behavior of TiAl intermetallic compounds.

In this study, the role of He atoms on the formation and annihilation process of radiation-induced defect clusters is

* Corresponding author. Tel.: +81-294 235 771; fax: +81-294 236 952; e-mail: nakataki@hrl.hitachi.co.jp.

investigated for one of the fundamental studies on the mechanism of neutron irradiation damage in TiAl intermetallic compounds. A TiAl compound with a dual phase of γ -TiAl and α_2 -Ti₃Al is selected for the test material because of its good ductility.

2. Experimental procedure

A Ti-rich TiAl compact was used. The compact shows a fairly large tensile elongation of 6% at 873 K [8] and superplasticity above 1223 K [11]. The manufacturing process was as follows. Powders with 250 μm average diameter were prepared by a plasma rotating electrode process (PREP), using a Ti-47 at.% Al electrode [12–14]. A cylindrical compact, 60 mm in diameter and 100 mm long, was made by hot isostatic pressing (HIP) at 1423 K and 176 MPa for 10.8 ks. The compact was forged isothermally (IHF) with up to a 78% reduction in length with a strain rate of 3.8×10^{-4} /s at 1223 K in vacuum. The forging provided a homogeneous fine grain structure and no cracks were found in the compact. The chemical composition of the compact is given in Table 1; major impurities are O and N, which were mainly included in the original TiAl electrode. The sample contained duplex structures of γ -TiAl and α_2 -Ti₃Al with fine and equiaxial grains, and about 80% of the volume fraction was γ -TiAl grains and the remaining was α_2 -Ti₃Al grains. The average grain size was about 3 μm for the γ -TiAl grains.

Disks, 3 mm in diameter and 0.25 mm thick, were made by wire cutting. The disks were electropolished into foils by a twin jet technique in a solution of 5% perchloric acid and 95% methyl alcohol at about 268 K for irradiation with electrons or He-ions.

The electron irradiation and microstructure observations were carried out in a high voltage electron microscope operated at 1 MV. The irradiation flux measured with a Faraday cup was 3×10^{23} e/m²s, which corresponded to a damage rate of 1.4×10^{-3} dpa/s, assuming a threshold displacement energy of 25 eV [5]. With use of thickness fringes near the foil edge or on a grain boundary, areas about 600 nm thick were selected for irradiation. The irradiation temperature was controlled from 473 to 873 K by an electric heater. The electron irradiated sample was also observed using a 200 kV transmission electron microscope (TEM) to obtain higher resolution when necessary.

The irradiation with 200 keV He-ions was done with a Cockcroft ion accelerator. The irradiation was continued up to fluences from 1×10^{21} to 4×10^{21} ion/m² with a

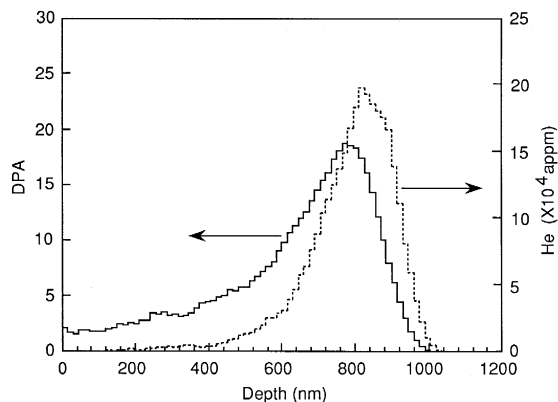


Fig. 1. Damage and stopped He profiles calculated by the TRIM85 code for the 200 keV He-ion irradiation to 3×10^{21} ions/m² in TiAl.

flux of 6×10^{17} ion/m²s at temperatures from 623 to 773 K in a vacuum of less than 2×10^{-4} Pa. The specimen temperature was controlled with an accuracy of 5 K during irradiation by an electric heater. The depth profiles of damage and stopped ions were calculated by the TRIM85 code [15] and are shown in Fig. 1 for the TiAl sample irradiated with 200 keV He-ions up to 3×10^{21} ion/m². The damage peak and stopped-ion peak were at depths of about 760 μm and 820 μm from the ion bombarded surface, respectively. Microstructural observation of He-ion irradiated samples was carried out at a depth of less than 200 nm and near the damage peak (about 700 nm in depth) of the samples. TEM foils for observation near the damage peak were prepared by 25 kV Ar-ion sputtering. The foil thickness was measured by the stereoscopic method. The average damage rate at a depth of less than 200 nm was estimated to be 6×10^{-4} dpa/s.

Some of the irradiated samples were annealed at temperatures from 673 to 1053 K for 0.72 to 1.8 ks in the 200 kV TEM. The annealing temperatures were controlled within 1 K.

3. Results

3.1. Defect clusters formed by electron or He-ion irradiation in TiAl and Ti₃Al grains

Fig. 2 consists of electron micrographs showing defect clusters produced in γ -TiAl grains by electron or He-ion irradiation at 623 K and 773 K. Dot-shaped clusters are formed by the irradiation at 623 K, and there is little difference between the microstructures of the samples irradiated with electrons and He-ions. However, a marked difference could be seen in the samples irradiated at 773 K. Many interstitial loops with stacking faults, lying on {111} planes, are formed by the He-ion irradiation at 773

Table 1

Chemical composition (at.%) of the material used

Al	Fe	Si	O	N	H	Ti
46.8	0.01	0.03	1.12	0.80	0.01	balance

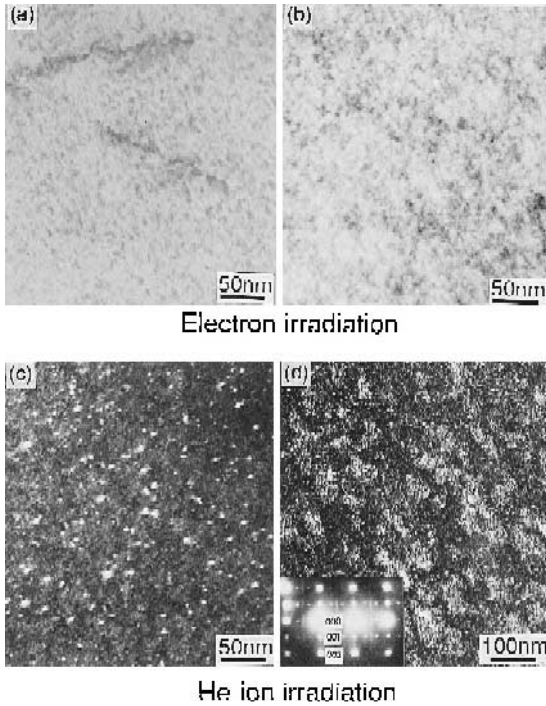


Fig. 2. Electron micrographs of TiAl grains irradiated with electrons and He-ions. (a) Bright field image after electron irradiation to 1.5 dpa at 623 K; (b) bright field image after electron irradiation to 2 dpa at 773 K; (c) dark field image after He-ion irradiation to 1 dpa at 623 K; (d) dark field image after He-ion irradiation to 3 dpa. The line contrast in (a) is corresponding to dislocations existing before irradiation.

K. The loop character was identified by the inner/outer method [5]. No clearly shaped clusters are observed in the case of electron irradiation. Extraspots streaking parallel to [001] appear in the electron diffraction pattern of both samples irradiated with electrons and He-ions at 773 K. One of the corresponding diffraction patterns is shown in Fig. 2(d) for the He-ion irradiated sample. This result suggests that a small amount of phases other than γ -TiAl is formed in TiAl grains during irradiation.

The dose dependences of density and average diameter of defect clusters are shown in Fig. 3 for TiAl irradiated with He-ions at 773 K and 623 K. The density increases rapidly at less than about 1 dpa, and then is saturated to be a constant value with higher doses. The average diameter, on the other hand, increases with increasing irradiation dose up to 4 dpa at 623 and 773 K. A similar tendency was also found in electron irradiated TiAl grains at temperatures from 473 to 673 K.

The saturation values of the cluster density are plotted against irradiation temperature in Fig. 4 for electron and He-ion irradiated TiAl and Ti_3Al grains. In TiAl grains irradiated with electrons, the saturation values show a slight temperature dependence from 473 to 673 K, and no

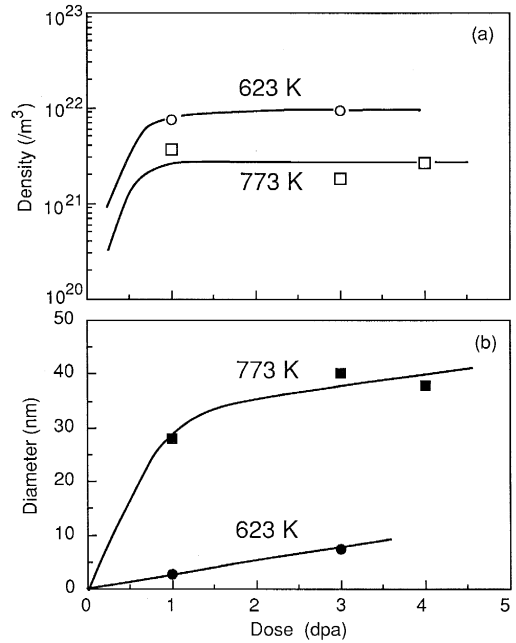


Fig. 3. Dose dependences of (a) defect cluster density and (b) average diameter in TiAl grains irradiated with He-ions at 623 and 773 K.

defect cluster formation is seen by TEM observations at 773 K and above. The density in TiAl grain irradiated with He-ions is almost one order of magnitude higher than that for electron irradiation at temperatures from 623 to 773 K. The difference in density between the He-ion and the electron irradiations is larger at the higher temperature. On

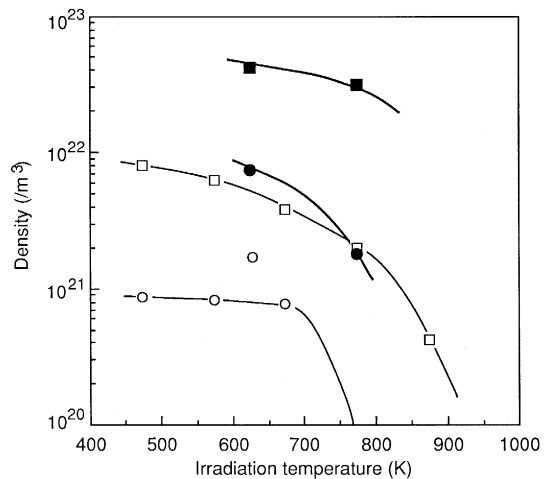


Fig. 4. Irradiation temperature dependences of saturated cluster density in TiAl and Ti_3Al grains irradiated with electrons or He-ions. \circ : TiAl grains irradiated with electrons, \bullet : TiAl grains irradiated with He-ions, \square : Ti_3Al grains irradiated with electrons, and \blacksquare : Ti_3Al grains irradiated with He-ions.



Fig. 5. Cavity structure in γ -TiAl and α_2 -Ti₃Al grains irradiated with He-ions to about 10 dpa at 773 K.

the other hand, the saturation densities in Ti₃Al grains are about five to ten times higher than those in TiAl grains for electron and He-ion irradiations. Moreover, faulted loops were formed on the (0001) plane in Ti₃Al grains irradiated with electrons at 773 and 873 K, although no defect clusters were formed in TiAl grains.

3.2. Formation of cavities

A cavity structure is shown in Fig. 5 for the sample irradiated with He-ions at 773 K. The structure was observed near the damage peak region of about a 700 nm depth from the ion bombarded surface, where the dose was estimated to be about 10 dpa from Fig. 1. Small cavities, about 3 nm in diameter, are formed in both TiAl and Ti₃Al grains. The cavity density in TiAl and Ti₃Al grains was 9×10^{21} and $2 \times 10^{22}/\text{m}^3$, respectively. The cavity formation seems to relate to injected He ions and vacancies [5]. Some of the cavities in TiAl grains appear in a

row. Dislocations that existed before irradiation would provide preferential nucleation sites, resulting in the formation of cavity rows. On the other hand, cavities were distributed randomly in Ti₃Al grains because there were few dislocations before irradiation. A lot of cavities are also seen along both γ - γ and γ - α_2 grain boundaries.

No cavities could be observed in electron irradiated samples up to 30 dpa at any irradiation temperature in the present study.

3.3. Annealing behavior of defect clusters and cavities

Annealing behavior of defect clusters was studied in the electron or He-ion irradiated TiAl grains. Fig. 6 shows the defect structures after annealing for 720 ks at various temperatures following the He-ion irradiation at 623 K to 1 dpa. Dot-shaped defect clusters of 7 nm in average diameter exist with a density of $8 \times 10^{21}/\text{m}^3$ in the as-irradiated sample. The number of defect clusters decreases during annealing, but their size seems to be unchanged. Nearly all clusters disappear at 873 K.

The change in cluster density caused by annealing is shown in Fig. 7 for samples irradiated with electrons and He-ions to 1 dpa at 623 K. The density is normalized by the respective as-irradiated value in the figure. Both annealing curves are in good agreement, although the initial density of the He-ion irradiated sample is several times higher than that of the electron irradiated one, as shown in Fig. 4. The dot-shaped clusters remarkably decrease in number around 800 K, and are annealed out completely at 900 K.

Fig. 8 shows microstructures in TiAl subsequently annealed at 873 K and 1053 K after the He-ion irradiation at 773 K. These observations were carried out in the region of about 3 dpa. Although interstitial loops hardly change by annealing at 873 K for 1.2 ks, new defects appear during the annealing. These defects were planar, lying

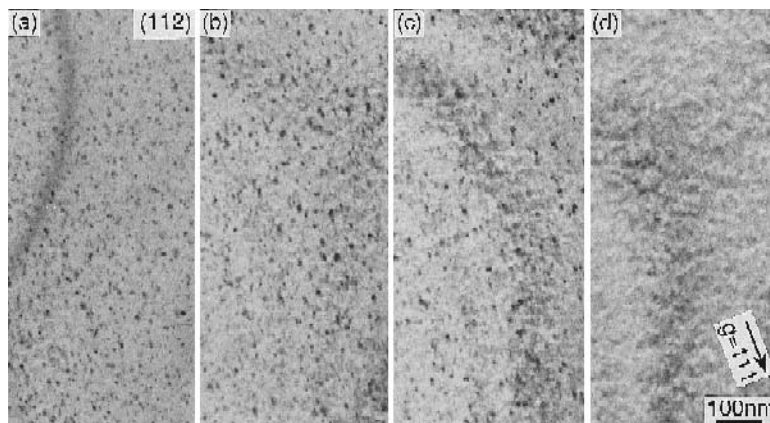


Fig. 6. Bright-field micrographs of TiAl grains irradiated with He-ions at 623 K to 1 dpa. (a) As-irradiated. After annealing for 720 s at (b) 673 K, (c) 773 K, and (d) 873 K.

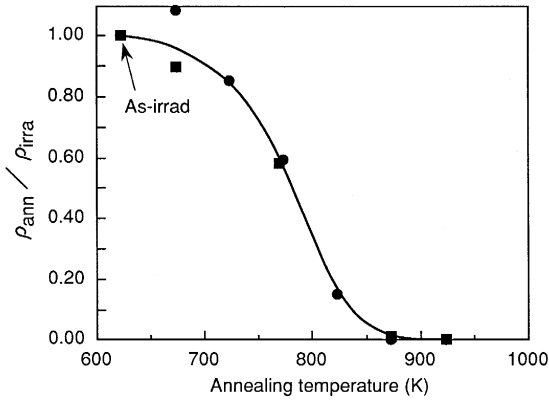


Fig. 7. Change in cluster density during isochronal annealing for TiAl irradiated with He-ions (■) and electrons (●) at 623 K to 1 dpa. The annealing was carried out for 720 s at each temperature. The cluster density (ρ_{ann}) was normalized by the value for each as-irradiated specimen (ρ_{irra}).

nearly on the (001) plane. From weak beam image analysis, the planar defects seemed to be stacking faults. Most of the interstitial loops disappeared after annealing at 1053 K for 1.2 ks. The planar defects grew slightly and still remained after the annealing.

The changes in cluster density and diameter by isochronal annealing are shown in Fig. 9 for TiAl irradiated with He-ions at 773, together with those in the sample irradiated at 623 K. Interstitial loops, produced by the irradiation at 773 K, decrease in number between 820 and 950 K. The average sizes of as-irradiated samples were 7 and 40 nm at irradiation temperatures of 623 and 773 K, respectively. The cluster size in the sample irradiated at 623 K was hardly changed by annealing below 773 K, and cluster shrinkage was observed above 800 K. Interstitial loops formed at 773 K showed no growth during annealing up to 850 K. The annealing behavior in TiAl was charac-

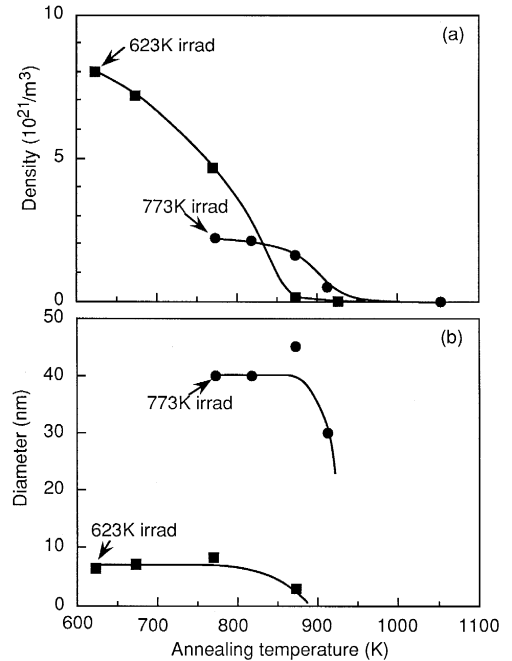


Fig. 9. (a) Changes in defect cluster density and (b) average diameter during isochronal annealing in He-ion irradiated TiAl grains. The specimen was originally irradiated at 623 K to 1 dpa or at 773 K to 3 dpa.

terized by no increase in cluster size during annealing. The cavity structures formed by He-ion irradiation at 773 K and annealed at 1053 K for 1.8 ks are shown in Fig. 10 for TiAl and Ti_3Al grains. The changes in cavity density and average diameter by annealing at 1053 K for 1.8 ks are shown in Fig. 11. The cavity densities after the annealing were 1.7×10^{22} and $3 \times 10^{21}/m^3$ in Ti_3Al and TiAl, respectively. The density was slightly lower than that in

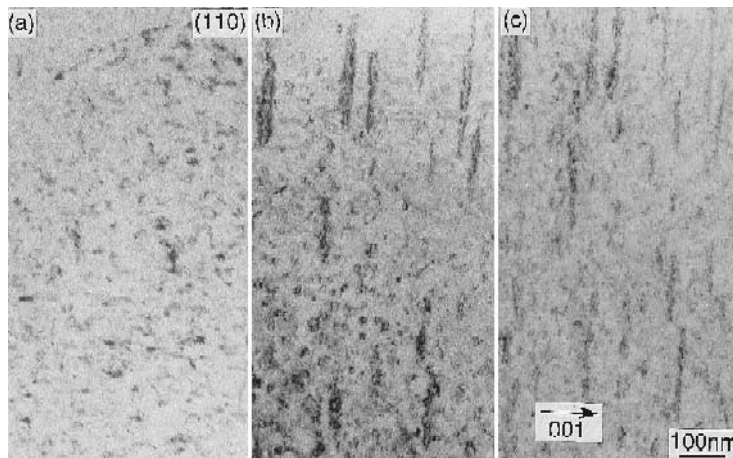


Fig. 8. Microstructures of TiAl grains irradiated with He-ions at 773 K to 3 dpa. (a) As-irradiated. After annealing for 1.2 ks at (b) 873 K, and (c) 1053 K.

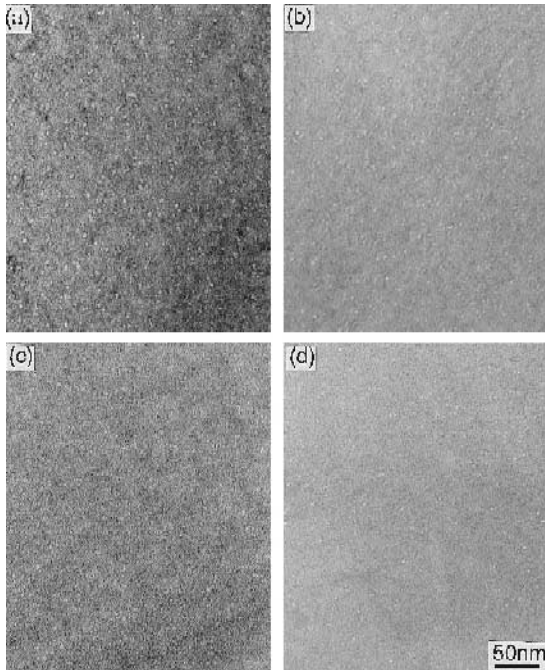


Fig. 10. Cavity structures of (a, c) as-irradiated and (b, d) after annealing at 1053 K for 1.8 ks in (a, b) Ti_3Al and (c, d) TiAl grains irradiated with He-ions at 773 K to about 10 dpa.

the as-irradiated samples, but the average diameter of cavity after annealing was almost the same as that in the as-irradiated Ti_3Al and TiAl .

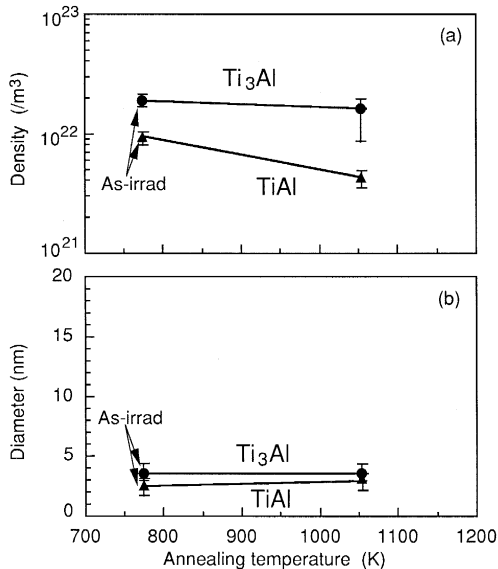


Fig. 11. (a) Changes in cavity density and (b) average diameter by the 1053 K annealing after He-irradiation at 773 K to about 10 dpa in TiAl and Ti_3Al grains.

4. Discussion

The cluster densities resulting from the He-ion irradiation were several times higher than those from electron irradiation in both TiAl and Ti_3Al grains, as shown in Fig. 4. Interstitial loops with stacking faults were formed by the He-ion irradiation at 773 K in TiAl , although no defect clusters were found after the electron irradiation. The difference in the formation of defect clusters may be attributed to the difference in defect production rates of He-ion and electron irradiation. In this study, the damage rates of He-ion and electron irradiations were slightly different: about 6×10^{-4} and 1.4×10^{-3} dpa/s, respectively. But such a difference in damage rates between the two irradiations is not significant enough to explain the difference in the formation of defect clusters. The defect clusters of the sample irradiated with He-ions were observed in the region less than a 200 nm thickness of the irradiated foils. A large amount of He ions penetrate the region, but He atoms with a concentration of more than 1000 ppm are present in the region, according to the result of the TRIM85 calculation (cf. Fig. 1). Moreover, He atoms have been detected by EELS analysis in the region [5]. From this consideration, the enhancement of the interstitial loop formation under the He-ion irradiation is attributed to the injected He atoms.

In order to confirm the effect of He atoms on defect cluster formation, He pre-injected TiAl grains were irradiated with electrons at 623 and 773 K. The He pre-injection was carried out by He-ion irradiation at 623 K to about 300 ppm in the sample. After electron irradiation to 4.5 dpa at 773 K, many loops with 50 nm in average diameter were observed, as shown in Fig. 12. These loops included stacking faults and lay on $\{111\}$ planes, which were of the same type as the interstitial loops formed by He-ion irradiation at 773 K (Fig. 2). A lot of interstitial loops were also observed under the electron irradiation at 623 K to 1.1 dpa, as also shown in Fig. 12, although only dot-shaped clusters

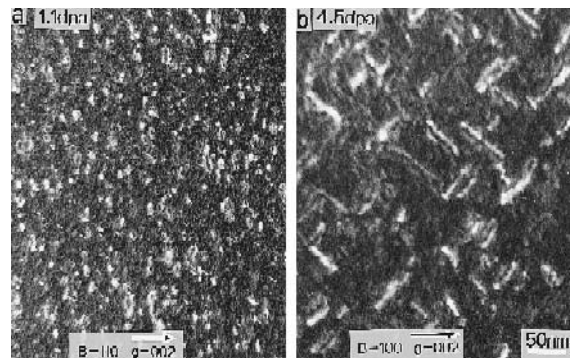


Fig. 12. Effect of pre-injected He atoms on electron irradiation microstructure in TiAl at (a) 623 K and (b) 773 K. He pre-injection was performed at 623 K, and the He concentration in the electron irradiated areas was calculated as about 300 appm.

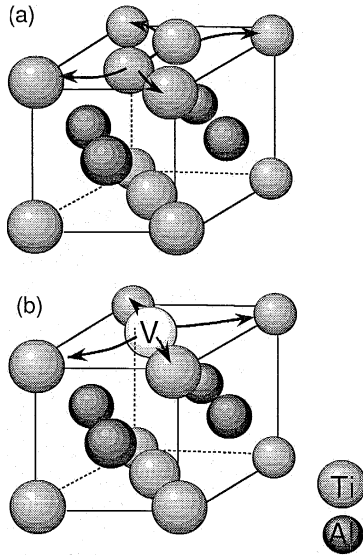


Fig. 13. Jump directions of (a) a [100] dumbbell and (b) a vacancy predicted in the $L1_0$ ordered structure of TiAl.

were formed in the non-He pre-injected sample (Fig. 2). These facts clearly indicate that He atoms enhance the formation of interstitial loops in TiAl intermetallic compounds.

TiAl has the $L1_0$ ordered crystal structure, and its antiphase boundary (APB) energy has been reported to be very high [16,17]. A [100] dumbbell interstitial migrates only on the (001) plane, with four jump directions in order to keep the ordered structure, as shown in Fig. 13. A vacancy may migrate in similar directions, as also shown in Fig. 13. If the jumps occurred in other directions, anti-site defects would be created. The defect migration to produce anti-site defects is not energetically favorable. Limited diffusion paths for irradiation-induced defects have also been predicted from recent theoretical and experimental works in a Ni_3Al alloy with the $L1_2$ ordered structure [18,19].

Petouhoff et al. [7] measured the long-range order parameter in TiAl irradiated with Ar-ions to 5 dpa at

relatively lower temperatures of 98–138 K, and observed disordering under the irradiation. In the present study, no irradiation-induced disordering was observed in TiAl irradiated with He-ions up to 10 dpa at 773 K, judging by superlattice reflection in electron diffraction of the samples. However, the injected He atoms would probably reduce the degree of order in TiAl, if they occupied substitutional sites in the lattice. Hence, migration of interstitials in He-injected TiAl may be somewhat easier than in non-He-injected TiAl. Higher interstitial mobility results in enhancement of defect cluster nucleation and a larger growth rate in He pre-injected and He-ion irradiated TiAl.

Cavities formed by He-ion irradiation at 773 K were not enlarged by annealing up to 1053 K for 1.8 ks in either TiAl or Ti_3Al . For comparison, type 316L stainless steel (Fe–12.4%Ni–16.9%Cr–2.2%Mo) was irradiated and annealed at nearly the same condition as the TiAl and Ti_3Al samples. The as-irradiated microstructure is shown in Fig. 14(a). Cavities, 4 nm in average diameter and with a density of $1.8 \times 10^{22}/m^3$, were formed by the irradiation. The density and diameter have nearly the same values as in TiAl and Ti_3Al . After annealing at 1023 K for 1.8 ks, the cavities enlarged to a size of 18 nm in average diameter, and some aligned themselves on residual dislocation lines (Fig. 14(b)). This result shows vacancies and He atoms migrate and aggregate during the annealing in type 316L stainless steel. The fact indicates that the mobility of vacancies and He atoms is much different between stainless steels and TiAl intermetallic compounds, which is caused by the ordered structures in TiAl intermetallic compounds.

5. Summary

In order to clarify fundamentally the role of He atoms on radiation damage in TiAl intermetallic compounds with a dual phase of γ -TiAl and α_2 - Ti_3Al , formation and annealing behavior of defect clusters in the TiAl compound irradiated with He-ions has been compared with that

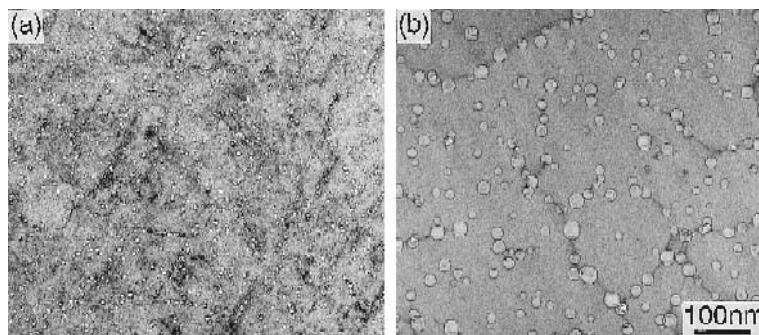


Fig. 14. Cavity structures in type 316L stainless steel irradiated with He-ions at 773 K to about 10 dpa. (a) As-irradiated and (b) 1023 K annealed for 1.8 ks.

in the sample irradiated with electrons. The main results are summarized as follows.

(1) The density of defect clusters formed by He-ion irradiation at temperatures from 623 to 773 K was about one order of magnitude higher than that of clusters formed by electron irradiation in γ -TiAl and α_2 -Ti₃Al grains.

(2) He atoms in TiAl intermetallic compounds enhanced the nucleation of defect clusters, especially interstitial loops, during irradiation.

(3) The dot-shaped clusters or interstitial loops did not grow during annealing, but most of them were annihilated by annealing up to 923 K in TiAl grains irradiated with He-ions and electrons. He atoms in TiAl grains had little influence on annealing of irradiation-induced clusters. The stacking faults, lying nearly on the (001) plane, appeared by annealing above 873 K in He-ion irradiated TiAl grains.

(4) Cavities were formed by He-ion irradiation to about 10 dpa at 773 K in both TiAl and Ti₃Al grains, while none were formed by electron irradiation up to 30 dpa. The cavities related to He atoms did not enlarge after annealing at 1053 K for 1.8 ks.

Acknowledgements

The authors are grateful to Professor M. Tokizane of Ritsumeikan University for helpful discussions, and also to Dr T. Aruga of JAERI for his help and comments on calculations using the TRIM85 code.

References

- [1] M. Matsuo, ISIJ Int. 31 (1991) 1212.
- [2] S. Mori, H. Miura, S. Yamazaki, T. Suzuki, A. Shimizu, Y. Seki, T. Kunugi, S. Nishino, N. Fujisawa, A. Hishinuma and M. Kikuchi, Fusion Technol. 21 (1992) 1774.
- [3] A. Hishinuma, J. Plasma Fusion Res. 70 (1994) 719.
- [4] A. Hishinuma, K. Nakata, K. Fukai, K. Ameyama and M. Tokizane, J. Nucl. Mater. 199 (1993) 167.
- [5] K. Nakata, K. Fukai, A. Hishinuma, K. Ameyama and M. Tokizane, J. Nucl. Mater. 202 (1993) 39.
- [6] E.M. Grala and J.B. McAndrew, in: Mechanical Properties of Intermetallic Compounds, ed. J.H. Westbrook (Wiley, New York, 1960) p. 229.
- [7] N.L. Petouhoff, A.J. Ardell, W.C. Oliver and B.N. Lucas, in: Structural Intermetallics, eds. R. Darolia, J.J. Lewandowski, C.T. Liu, P.L. Martin, D.B. Miracle and M.V. Nathal (The Minerals, Metals and Materials Society, USA, 1993) p. 77.
- [8] A. Hishinuma, K. Fukai, T. Sawai and K. Nakata, Intermetallics 4 (1996) 179.
- [9] A. Koyama, T. Yamada, M. Ogawa, H. Matsui and M. Narui, Proc. of the 2nd Japan/China Sym. on Materials for Advanced Energy Systems and Fission and Fusion Engineering (The University of Tokyo, Japan, 1994) p. 472.
- [10] R.T. Santoro, ORNL-TM-5033 (1975).
- [11] T. Wajata, K. Isonishi, K. Ameyama and M. Tokizane, ISIJ Int. 33 (1993) 884.
- [12] M. Tokizane and R. Kumagaya, Proc. Int. Conf. on PM Aerospace Materials 1991 (MPR Publishing Services, UK, 1992) pap. 26-1.
- [13] M. Tokizane and K. Isonishi, J. Jpn. Soc. Powder Powder Metall. 39 (1992) 1137.
- [14] K. Ameyama, K. Isonishi, T. Wajata, T. Fujii and M. Tokizane, Proc. 3rd Jpn. Int. SAMPE Symp. (Chiba, Japan, 1993) p. 1513.
- [15] J.F. Ziegler, J.P. Biersack and U. Littmark, The Stopping and Ranges of Ions in Materials, Vol. 1 (Pergamon, New York, 1985).
- [16] D. Schectman, M.J. Blackburn and H.A. Lipsitt, Metall. Trans. 5 (1974) 1373.
- [17] E.L. Hall and S. Huang, Acta Metall. 38 (1990) 539.
- [18] A. Cao, M. Victoria and R.S. Averback, J. Mater. Res. 5 (1990) 1409.
- [19] T.X. Bui, I.M. Robertson, J.L. Klatt, R.S. Averback and M.A. Kirk, J. Nucl. Mater. 205 (1993) 312.